ISSN 1991–3966. Жидк. крист. и их практич. использ. / Liq. Cryst. and their Appl., 2020, 20 (3), 72–79

UDC 532.5, 532.6

D. V. Shmeliova, A. Sh. Saidgaziev, S. S. Kharlamov, A. S. Visotsky, M. A. Safonov, A. A. Konovalova, S. V. Pasechnik*

LIQUID CRYSTAL OPTOFLUIDIC DEVICE BASED ON ELECTRO-KINETIC PHENOMENA IN POROUS POLYMER FILMS

MIREA – Russian Technological University, Problem Laboratory of Molecular Acoustics,
78 Vernadsky Av., Moscow, 119454, Russia. *E-mail: s–p–a–s–m@mail.ru

In this paper we describe the first experimental realization of the previously proposed optofluidic liquid crystal device based on electro-osmotic flows arising in the porous polymer (PET) film filled with a nematic liquid crystal (NLC). These flows induced Poiseuille's shear flow of NLC through the plane channels with a hometropic orientation, which resulted in the flow induced modulation of the intensity of light, passed through the channels. The additional application of magnetic field provided the stabilization of the homeotropic orientation. The results of numerical calculations of hydrodynamic and optical characteristics of the device were compared with the experimental data.

Key words: *liquid crystal, optofluidics, light modulator, electrokinetic pump.*

DOI: 10.18083/LCAppl.2020.3.72

Д. В. Шмелева, А. Ш. Саидгазиев, С. С. Харламов, А. С. Высотский, М. А. Сафонов, А. А. Коновалова, С. В. Пасечник*

ЖИДКОКРИСТАЛЛИЧЕСКОЕ ОПТОФЛЮИДНОЕ УСТРОЙСТВО, ОСНОВАННОЕ НА ЭЛЕКТРОКИНЕТИЧЕСКИХ ЯВЛЕНИЯХ В ПОРИСТЫХ ПОЛИМЕРНЫХ ПЛЕНКАХ

МИРЭА – Российский технологический университет, Проблемная лаборатория молекулярной акустики,
пр. Вернадского, д. 78, 119454 Москва, Россия. *E-mail: s–p–a–s–m@mail.ru

В этой статье мы описываем первую экспериментальную реализацию ранее предложенного оптофлюидного жидкокристаллического устройства, основанного на электроосмотических потоках, возникающих в пористой полимерной (ПЭТ) пленке, заполненной нематическим жидким кристаллом (НЖК). Эти потоки индуцировали Пуазейлевский сдвиговый поток НЖК через плоские каналы с гомеотропной ориентацией, что привело к индуцированной потоком модуляции интенсивности света, проходящего через каналы. Дополнительное приложение магнитного поля обеспечивало стабилизацию гомеотропной ориентации. Результаты численных расчетов гидродинамических и оптических характеристик устройства сопоставлены с экспериментальными данными.

Ключевые слова: *жидкий кристалл, оптофлюидика, модулятор света, электрокинетический насос.*

Introduction

The wide application of liquid crystals (LC) in display industry is based on electro-optical effects, which originate due to changes of the initial orientation of a local optical axis (director) under action of electric field. For the last decades, many ideas and technical solutions concerning possible applications of liquid crystals in different photonic devices and sensors were proposed [1, 2, 3]. Electric fields for the control of optical properties of LC in some types of such devices meet the serious problems, which can be overcome by usage of new methods of manipulation with liquid crystal properties. One of the basic property of liquid crystals is change of the initial orientation under action of shear flows [1]. The investigations of mechano-optical properties of liquid crystals has a long history [1, 5], but only nowadays they were realized on the base of a microfluidic chip, which made possible to announce about the new class of LC devices – optofluidic devices [6]. Such devices can be used as light modulators for different ranges of optical irradiation – visible and near infrared, for example. Recently, it was pointed out that application of mechano-optical phenomena attracts a special interest for elaboration of LC devices operating in THz range – terafluidic LC modulators [7]. The standard schema for an electric control, used in LC displays, fails for THz range, in particular due to big energy losses in ITO electrodes. So, alternative variants to control the THz irradiation via LC elements, for example with the help of magnetic fields [8, 9] were proposed. In the latter case, the initial orientation of LC layer was changed due to magnet rotation respectively to the LC cell, which resulted in modulation of the intensity of THz wave, propagating through the liquid crystalline layer. Usage of shear flows instead of (or additionally to) magnetic fields can be considered as promising approach to elaboration of LC modulators operating in THz range. Recently, it was shown [10], that application of relatively low DC electric voltage (5…30 V) to the thin (23 μm of thickness) polymer (PET) porous films induced rather intensive electro-osmothic flows. It made possible to propose a new type of opto-fluidic LC modulator, which includes electro-hydrodynamic (EHD) pump producing electro-osmothic flows, and a number of the plane channels with the given initial orientation [4]. The technical characteristics of the modulator were estimated taking into account the previously obtained experimental data on electro-kinetic phenomena in polymer porous films filled with LC [10]. In this paper, we describe the first prototype of such device and present the experimental results, which are compared with the theoretical predictions.

Experimental

The design and operating principles of the optofluidic device, realized in this work is illustrated by Fig. 1, *a*.

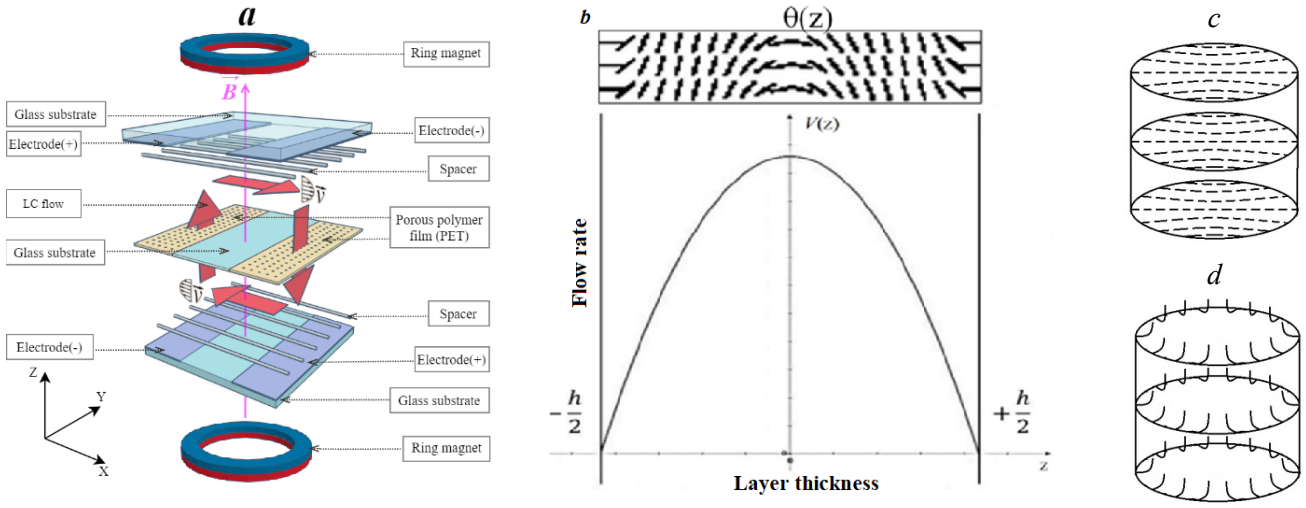

Fig. 1. a – Design and operating principle of optofluidic cell; *b* – profiles of velocity *v* and orientation θ; planar polar (PP) (*c*), and escaped radial (ER) (*d*) director configurations formed inside a pore

The device consists of two EHD pumps located at the terminal parts of LC cell and two plane capillaries formed in the central part of the cell. Each EHD pump includes a sample of porous PET film (of thickness d_1 = 23 μm and area S = 1.5 cm^2) with a large number $N = N_0S$ ($N_0 = 8.10^7$ cm^{-2} – the pores' density) of identical submicron open pores of diameter $D = 2R$ = 0.5 μm, oriented along the normal to the film plane. The film is located between two ITO electrodes needed to create an electric field after application of DC or low frequency AC voltage. The total distance between electrodes d is about 300 μm. The samples of the films are connected by glue with the central glass substrate (180 μm of thickness). Usage of cylindrical spacers makes it possible to form two plane capillaries with fixed gap h = 52 μm, length L = 1 cm and width A = 1.5 cm. The inner surfaces of the substrates were preliminary coated by a thin layer of chromium stearyl chloride (chromolane) to provide a homeotropic surface orientation of LC. Afterwards, the cell was vacuumed and filled with a nematic liquid crystal (NLC) 5CB (4-cyano-4'-pentylbiphenyl). The cell was fixed between two permanent neodymium ring-like magnets creating magnetic field of the induction B equal to 0.21 ± 0.05 T in the central region of a diameter 2mm illuminated by the laser beam (λ = 650 nm). Afterwards the cell was mounted on the optical bench and placed between crossed polarizers oriented at the angle 45^0 relatively the direction of LC flow through the plane channels. The application of DC electric voltage U to the EHD pumps induced Poiseuille's shear flow of NLC through the plane channels with the profile $v(z)$, shown in Fig. 1, *b*. As a result, the initial homeotropic orientation was distorted by the flow. The corresponding profile of a polar angle $\theta(z)$ is shown in Fig. 1, *b*. In turn, it induced birefringence and corresponding changes of the light intensity I, which were registered by a photodiode and passed to PC via AD convertor. The processing of the signal passed to PC was performed with the help of special software.

Results and discussion

The time dependences of the light intensity $I(t)$ at different DC voltages are shown in Fig. 2.

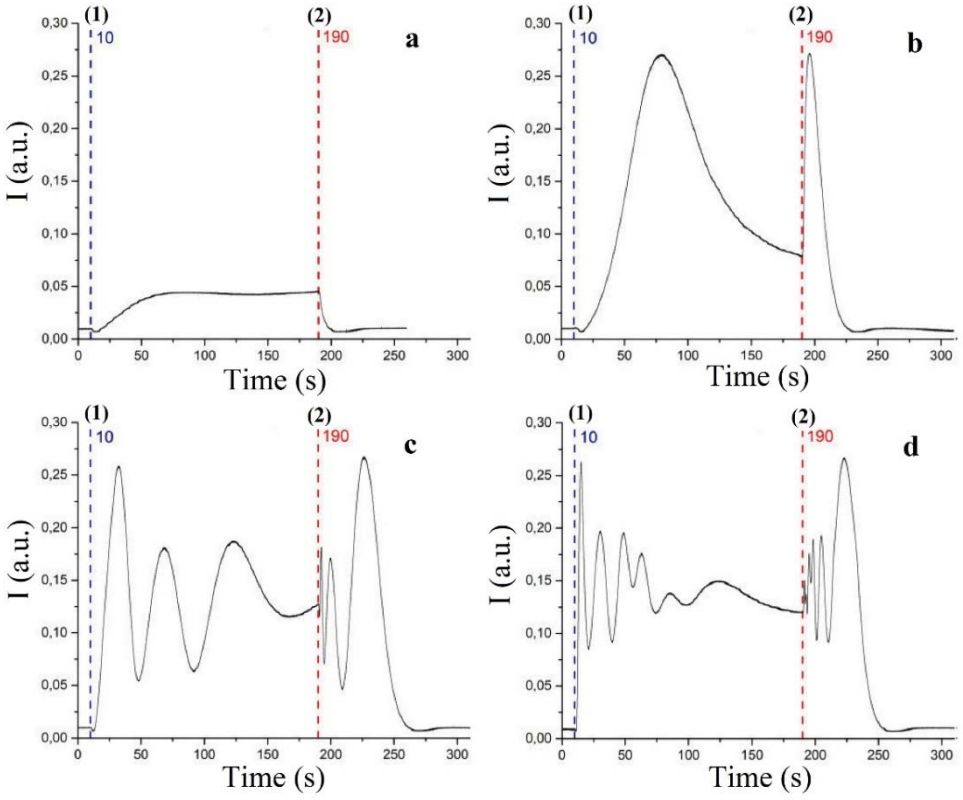

Fig. 2. Dependences of the light intensity I on time at different voltages U: *a* –3 V, *b* –5 V, *c* –10 V, *d* –15 V (1 – turning on electric field; 2 – turning off electric field)

The monotonic increasing of this parameter, observed after application of a relatively low voltage (Fig. 2, *a*), was transformed to more complicated form with a number of deep local minima and maxima (Fig. 2, *b,* 2, *c*). Previously, the similar oscillations were observed for the optical response of homeotropic LC layer on the applied quasi stationary decay flow of a low intensity which induced the director's reorientation in the plane of the flow [1]. The further increasing of the applied voltage (Fig. 2, *d*) resulted in smoothing the oscillations, which could be assigned to the first hydrodynamic instability – the escape of a director from the flow plane [1]. At higher voltages the secondary hydrodynamic instabilities were induced and visualized as the long living areas of quasi planar orientation, similar to those observed in a decay flow [1].

For comparison of the experimental results with the theoretical predictions, we used previously published [4] hydrodynamic model of EHD liquid crystal pump which induced Poiseuille's shear flows in a number of the plane channels, connected with the pump to create a circular motion of a liquid. The equivalent scheme, correspondent to the modified variant of this model, includes internal part (consisting of the two EHD pumps) with the internal hydrodynamic resistance Z_i, and the external part (consisting of the two plane channels) with the external hydrodynamic resistance Z_e. The values of Z_i and Z_e are expressed as:

$$Z_i = \frac{8d_1\eta}{N_0 * S * \pi * R^4} \quad (1)$$

$$Z_e = \frac{12L}{A * h^3} * \eta_1, \quad (2)$$

where η and η_1 – are the shear viscosities of LC inside pores and flat channels, correspondingly.

In the original version of the model, we considered the case when the external hydrodynamic resistance is essentially smaller than the internal one ($Z_e << Z_i$). In this case, the total flow rate Q_0 through the plane channels depended only on the pump parameters. Nevertheless, our estimation of the LC cell parameters presented above with usage of material coefficients of 5CB [12] showed that this strict inequality does not hold. Therefore, the modification of the model was performed to made calculations for arbitrary values of the ratio $r = Z_e/Z_i$. In this case, the total flow rate Q depends on the ratio r:

$$Q = \frac{Q_0}{(1+r)}, \quad (3)$$

where $Q_0 = Q(r = 0)$ – the flow rate for $Z_e << Z_i$, which can be calculated using the expression [10]:

$$Q_0 = N_0 S Q_i \quad (4)$$

In equation (4) Q_i is the flow rate through each pore, which is defined for a plug like velocity profile as:

$$Q_i = -(\varepsilon_0 * \varepsilon * \zeta)\left(\frac{\pi * R^2}{\eta}\right) * E, \quad (5)$$

where ε is the dielectric permittivity, ζ is the zeta potential.

So, the volume flow rate and other parameters of the flow through the plane channels depend both on external and internal parts of the model. One has to make some assumptions to apply the theoretical expressions presented above for analysis of experimental data. In particular, the strength of electric field may be different inside PET film pores and liquid crystal layers formed between porous film and glass substrates. This difference can be estimated by considering the capacitor model consisting of two dielectric layers (1 and 2) of different thickness (d_1 and d_2) with the different effective values (ε_1 and ε_2) of a dielectric permittivity ε. In the framework of this model, the expression for the electric field strength E_1 inside the film reads as:

$$E_1 = \frac{U}{d\left[\beta + \frac{\varepsilon_1}{\varepsilon_2}(1-\beta)\right]} = \alpha E_0, \quad (6)$$

where

$$E_0 = \frac{U}{d} \quad (7)$$

the electric field strength in the case of homogeneous media between the electrodes,

$$d = d_1 + d_2, \quad \beta = \frac{d_1}{d}. \quad (8)$$

In expression (8), d – the distance between ITO electrodes, d_1 – the thickness of the porous film, d_2 – the total thickness of two LC layers between the film and electrodes. In our case, the calculation results of E_1 depend on the LC orientational structures inside and outside porous film.

It is well known that different types of director distribution can be realized inside cylindrical cavities depending on the LC material parameters, boundary conditions and cavity diameter. Previously, we considered two types of orientational configurations formed inside a pore (Fig. 1, *c* and *d*) at homeotropic surface orientation. For the planar polar (PP) configuration, shown in Fig. 1, *c* the director's field lies in the plane of the film. In this case, the value of the dielectric permittivity ε of LC inside a pore is independent on space coordinates, and equals to the main value $\varepsilon_\perp = 7$ for 5CB. The theoretical expression (5) is valid for an isotropic polar liquid with a constant value of the dielectric permittivity, which is similar to the case of PP configuration and it makes possible to use the mentioned above value of ε for calculations presented below. The value of the dielectric permittivity ε_1 of composite media PET – LC can be estimated in accordance with an additive schema [9] as:

$$\varepsilon_1 = \varepsilon_{LC} * P + \varepsilon_{PET} * (1 - P). \qquad (9)$$

The estimation for $\varepsilon_{LC} = 7$, $\varepsilon_{PET} = 3.1$ and $P = 0.16$ gives the value $\varepsilon_1 = 3.72$.

The dielectric permittivity effective value ε_2 for the liquid crystal layers between porous film and electrodes depends on the LC orientation in these layers. One can expect a number of defects in the absence of electric field due to inhomogeneity of the planar orientation on PET surface and relatively large (about 150 μm) thickness of each LC layer. Application of electric field results in stabilization of a homeotropic orientation imposed by coatings of electrodes, except for the surface layers near PET film of thickness close to the electric coherence length ξ_E, which is defined as:

$$\xi_E = \sqrt{\frac{K_{11}}{\varepsilon_0 \Delta\varepsilon}} \frac{1}{E_0}, \qquad (10)$$

where K_{11} – the Frank's elastic module, $\Delta\varepsilon = \varepsilon_{II} - \varepsilon_\perp$, – the dielectric permittivity anisotropy equal to 11 for 5CB. The estimate made in accordance with (8) at voltage $U = 10$ V gives the value $\xi_E = 8$ μm, which is essentially smaller than the total thickness of LC layer (150 μm). It makes possible to use the value of a dielectric permittivity $\varepsilon_2 = \varepsilon_{II} = 18$ to estimate, accordingly to the equation (6), the corresponding parameter $\alpha = 3.75$ (the close value $\alpha = 3.6$ was found at the direct simulation of the problem using Comsol Multiphysics software).

The second escaped radial (ER) configuration shown in Fig. 1, *d* is characterized by the inhomogeneous declination of the director from the plane of the film, which results in the dependence of ε on the radial coordinate. It was shown [13], that for typical value of the anchoring strength about 3,5 J/m^2 and the submicron values of the pore's diameter, the weak anchoring effects played the essential role resulting in declination of the polar angle at boundary θ_R from the value $\pi/2$ (homeotropic boundary orientation) to the value $\theta_R \sim 55^0$. The estimation of the corresponding parameter ε, defined as:

$$\varepsilon = \frac{\varepsilon_\perp \varepsilon_\parallel}{\varepsilon_\perp cos^2\theta_R + \varepsilon_\parallel sin^2\theta_R} \qquad (11)$$

gives the value $\varepsilon = 9{,}5$, which can be used for calculation of the flow rate (expression (5)). In accordance with the expressions (7) and (6), it results in the values $\varepsilon_1 = 4.12$ and $\alpha = 3.43$.

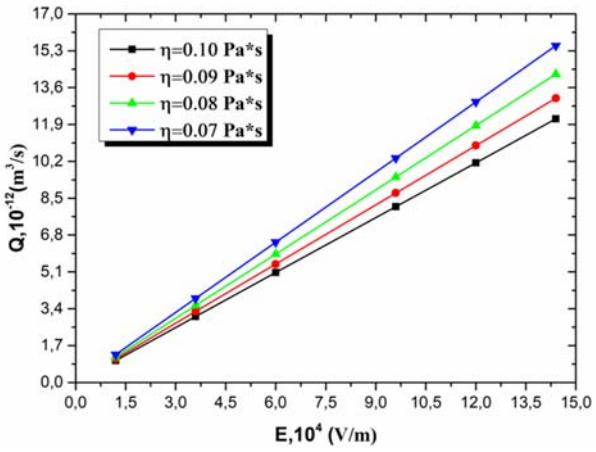

Fig. 3. The flow rate *Q* as function of the electric field strength *E* for different values of the shear viscosity η

The calculation results of the flow rate *Q* as a function of the electric field strength *E* are shown in Fig. 3 at different values of shear viscosity η inside a pore with PP configuration. As the effective shear viscosity of LC flowing through the plane capillary, the maximal value of the shear viscosity coefficient of 5CB $\eta_1 = 0.105$ Pa*s [12] was used. It is valid for the small flow induced distortions of the initial homeotropic orientation.

Usage of the data, presented in Fig. 3 makes possible to estimate the flow induced orientation changes and corresponding birefringence in the plane layers of LC. For this aim, we apply the previously proposed model for a linear response of a homeotropic layer of LC on the low frequency oscillations of a pressure gradient G in the presence of electric field [1]. In the case of the quasi-stationary shear flow realized in our experiments, the director follows the pressure gradient without phase lag and the flow-induced distortion of the polar angle θ is described by the following simplified expression:

$$\theta(\tilde{z}) = \frac{-G*h}{\eta_1*\omega_b} * \left(\tilde{z} + \frac{e^{k_1\left(\tilde{z}-\frac{1}{2}\right)}+e^{-k_1\left(\tilde{z}-\frac{1}{2}\right)}}{2e^{k_1}+2e^{-k_1}-4} - \frac{e^{k_1\left(\tilde{z}+\frac{1}{2}\right)}+e^{-k_1\left(\tilde{z}+\frac{1}{2}\right)}}{2e^{k_1}+2e^{-k_1}-4}\right), \quad (12)$$

where $\tilde{z} = z/h$, G – pressure gradient, which can be derived using equation:

$$G = \frac{Z_e Q}{L} \quad (13)$$

η_1 – Miesowicz coefficient, which defines the shear viscosity corresponding to the hometropic orientation of LC, k_1 – the wave number defined by the expression:

$$k_1 = \sqrt{\frac{{\mu_0}^{-1} * \Delta\chi * B^2 * h^2}{K_{33}}}, \quad (14)$$

K_{33} – Frank's elastic modulus, $\Delta\chi$ – anisotropy of magnetic susceptibility, ω_b – the frequency of the director's motion in the presence of a strong magnetic field, expressed as:

$$\omega_b = \frac{{\mu_0}^{-1} * \Delta\chi * B^2}{\gamma_1}, \quad (15)$$

where γ_1 – rotational viscosity.

The calculations results of the polar angle $\theta(z)$ made in accordance with (12) have shown that the value of this parameter does not exceed $\pi/4$ throughout the layer. It means that the mentioned above linear approximation holds in the range of parameters used in calculations.

The obtained distribution of the polar angle $\theta(z)$ can be used to calculate the flow induced phase delay δ between the extraordinary ray (refractive index n_e = 1.73) and the ordinary one (refractive index n_o = 1.54) propagating through two plane layers of LC in accordance with the expression:

$$\delta = \frac{4 * \pi * h}{\lambda} * \frac{n_0(n_e^2 - n_0^2)}{2n_e^2} * \langle\Theta^2\rangle, \quad (16)$$

where the averaged value of the squared angle θ(z) is defined as:

$$\langle\Theta^2\rangle = \int_{\frac{-1}{2}}^{\frac{1}{2}} (\Theta)^2 d\tilde{z}. \quad (17)$$

The calculated dependences of the phase delay on the electric field's strength E for the PP configuration at different values of η are shown in Fig. 4.

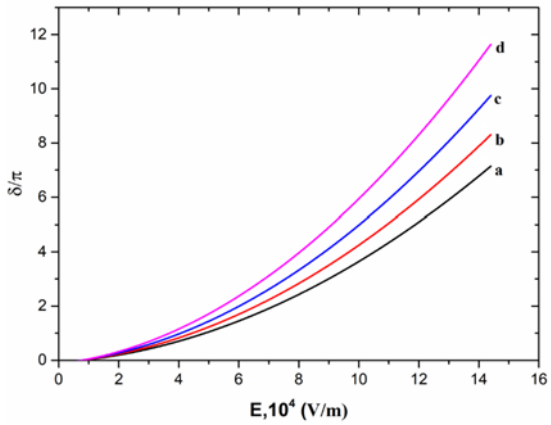

Fig. 4. The phase delay δ as function of the electric field strength E at different shear viscosities: a – η = 0.10 Pa*s, b – η = 0.09 Pa*s, c – η=0.08 Pa*s, d – η=0.07 Pa*s

It is possible to compare the calculation results of the phase delay δ with the experimental data taking into account the equations (6) and (7). The time dependences of the light intensity $I(t)$, shown in Fig. 2, *a-c* were processed to determine the stationary values of the flow induced phase delay δ_e in accordance with the next expression:

$$I = I_0 sin^2 \frac{\delta_e}{2}, \quad (18)$$

where I_0 – the maximal intensity of light, taking place at $\delta_e = \pi n$.

The result of the comparison of the theoretical and experimental dependences of the phase delay on electric voltage is shown in Fig. 5.

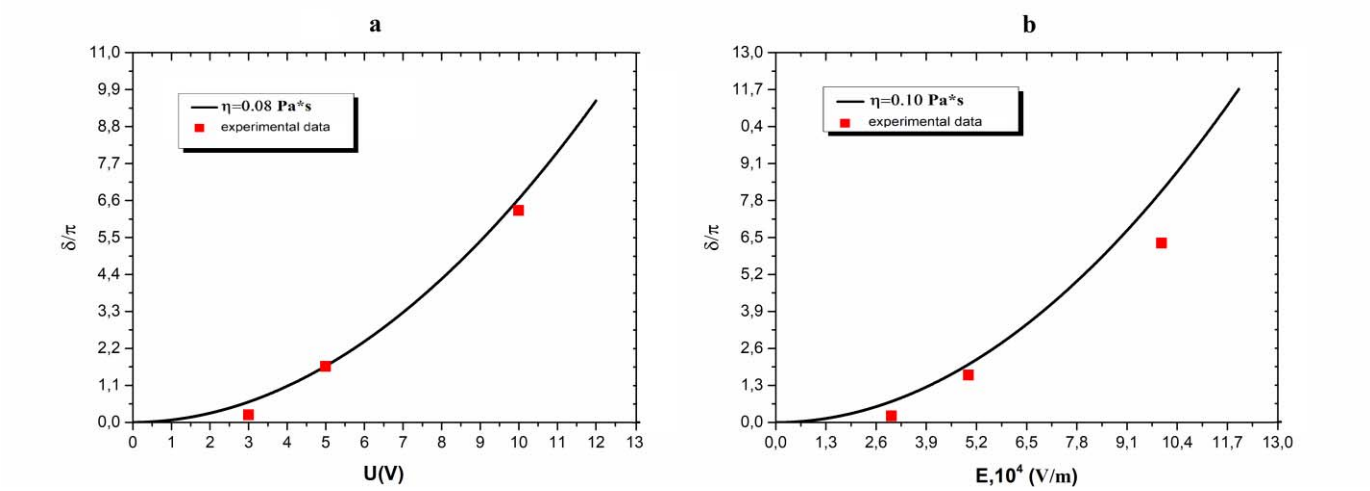

Fig. 5. Comparison of the theoretical dependences of phase delay δ on voltage U with the experimental data δ_e: *a* – planar polar configuration; *b* – escaped radial configuration

The best agreement between theory and experiment for PP configuration takes place at the value η = 0.08 Pa*s. It seems to be reasonable according to the flow geometry for this configuration. Indeed, the value of the effective shear viscosity may be in the range η_3 = 0.032 Pa.s < η <η_1 = 0.105 Pa*s., where η_3 – the third Miesowicz coefficient corresponding to the normal orientation of a director relatively to the flow plane. At the same time, the direct measurements of the effective shear viscosity in the same system made via Poiseuille's flow technique [13–15] gave the value about 0.04 Pa*s. The difference between two values of η may be partially explained by the principal difference between Poiseuille's flow with a parabolic velocity profile and electroosmotic flow with a plug-like profile. The results of similar calculations for ER configuration is shown in Fig. 5, *b*. The best agreement between theory and experiment takes place at η = 0.10 Pa*s. This value seems to be too high taking into account the mentioned above declination of polar angle from π/2. The estimations for the escaped radial configuration with point defects (ERPD), which may improve the agreement, are out of scope of this paper.

Conclusion

The first results of experimental investigation and computer modeling of optofluidic liquid crystal device are presented. The device is based on integrated liquid crystal cell composed of two electrohydrodynamic pumps, which provide a shear flow of a liquid crystal through two plane capillaries playing the role of the flow controlled light modulator. The optical response of LC on shear flow in the presence of magnetic field at different controlled voltages was registered and analyzed in the framework of proposed model. The satisfactory agreement of the experimental data and results of numerical calculations was established. It makes possible to predict the operation of such devices as modulators of electromagnetic waves of different frequencies, including IR a THz ranges.

Acknowledgements: *This work was supported by Ministry of Education and Science of Russian Federation (Grant № FSFZ-2020-0019). The reported study also was funded by Russian Foundation for Basic Research (RFBR and DFG project № 20-52-12040, and RFBR, project № 19-32-90055\19).*

References

1. Pasechnik S.V., Chigrinov V.G., Shmeliova D.V. Liquid Crystals: Viscous and Elastic Properties in Theory and Applications. New York: Wiley, 2009, 436 p.
2. Chigrinov V.G., Kozenkov M.V., Kwok H.S. Photoalignment of Liquid Crystalline Materials: Physics and Applications. John Wiley & Sons, 2008, 248 p.
3. Chigrinov V.G. Photoalignment and photopatterning: New liquid crystal technology for displays and photonics. *Fine Chemical Technologies*, 2020, **15** (2), 7–20.
4. Pasechnik S.V., Shmeliova D.V., Dubtsov A.V., Trifonov S.V., Chigrinov V.G. Electrically induced shear flows of liquid crystals confined to porous polymer films for Thz application. *Liq. Cryst. and their Appl*., 2018, **18** (1), 79–83.

5. Kapustin A.P., Kapustina O.A. Akustika zhidkih krtistallov. Moscow : Nauka, 1986, 250 p.
6. Cuennet J.G., Vasdekis A.E., De Sio L., & Psaltis D. Optofluidic modulator based on peristaltic nematogen microflows. *Nature Photonics*, 2011, **5** (4), 234–238.
7. Pasechnik S.V., Shmeliova D.V. Terafluidic devices: Perspectives and Problems. *IEEE 40th International Conference on Infrared, Millimeter and Terahertz Waves*, Hong Kong, 2015.
8. Ci-Lin Pan, Ru-Pin Pan. Recent progress in liquid crystal THz optics. *Liquid Crystal Materials, Devices, and Applications* XI, 2006, 6135, 61350 D.
9. Chen C.Y., Pan C.L., Hsieh C.F., Lin Y.F., & Pan R.P. A liquid-crystal-based terahertz tunable Lyot filter. *Appl. Phys. Lett*, 2006, **88** (10), 101107.
10. Pasechnik S.V., Chopik A.P., Shmeliova D.V., Drovnikov E.M., Semerenko D.A., Dubtsov A.V., Zhang W., Chigrinov V.G. Electro-kinetic phenomena in porous PET films filled with liquid crystals. *Liquid Crystals*, 2015, **42** (11), 1537–1542.
11. Pasechnik S.V., Krekhov A.P., Shmeleva D.V., Nasibullaev I.Sh., Tsvetkov V.A. Orientational instability in a nematic liquid crystal in a decaying Poiseuille flow. *J. Exp. Theor. Physics*, 2005, **100** (4), 804–810. **DOI:** 10.1134/1.1926441.
12. Stewart I. W. The static and dynamic continuum theory of liquid crystals. New York: Taylor and Francis Inc., 2004, 351 p.
13. Pasechnik S.V., Shmeliova D.V., Torchinskaya A.V., Semina O.A., Dyukin A.A., Chigrinov V.G. Rheological properties of liquid crystals in porous polymer films with submicron sizes of pores. *Liq. Cryst. and their Appl.*, 2016, **16** (4), 52–58. **DOI:** 10.18083/LCAppl.2016.4.52.
14. Pasechnik S.V., Shmeliova D.V., Kharlamov S.S., Semina O.A., Saidgaziev A.Sh., Chigrinov V.G. Electrorheology of liquid crystals. *Liq. Cryst. and their Appl.*, 2018, **18** (3), 89–93. **DOI:** 10.18083/LCAppl.2018.3.89.
15. Pasechnik S.V., Shmeliova D.V., Torchinskaya A.V., Semina O.A., Dyukin A.A. Method of decaying flow in rheology of polymeric porous films filled by liquid crystals. *Russian technological journal*, 2017, **5** (5), 25– 39.

Поступила 15.07.2020 г.
Received 15.07.2020
Принята 31.08.2020 г.
Accepted 31.08.2020